On the lifetimes of Rydberg states probed by delayed pulsed field ionization

F. Merkt and R. N. Zare
Department of Chemistry, Stanford University, Stanford, California 94305-5080

(Received 11 April 1994; accepted 19 May 1994)

We present a simple model to evaluate the degree of l and m_l mixing in high Rydberg states that results from perturbations caused by weak, homogeneous dc electric fields and static ions. This model predicts the lifetime of these states qualitatively and explains several seemingly contradictory observations obtained using zero-kinetic-energy (ZEKE) photoelectron spectroscopy. The presence of a small homogeneous dc electric field and a few ions in the sample volume causes m_l mixing in general as well as l mixing, both of which contribute to the lengthening of the lifetimes. Consequently, the lifetime lengthening appears to be insensitive to the sample pressure. The effect of the dc electric field on the lifetime is complex. Although the electric field results in l mixing, with increasing field strength it inhibits m_l mixing, and, at still higher field strength, induces ionization. The variation of the lifetimes with ion concentration is also complicated. At low ion concentration, the m_l mixing varies across the Stark manifold of Rydberg states that belong to the same principal quantum number, so that different states have different lifetimes. At higher ion concentration, l and m_l mixing are more uniform, which lengthens the lifetimes and makes them more similar across the Stark manifold. At still higher concentrations, collisional ionization dominates, which shortens the lifetimes.

I. INTRODUCTION

Over the past 10 years, the technique of zero-kinetic-energy (ZEKE) photoelectron spectroscopy has become established as a powerful tool to obtain high-resolution spectroscopic information on singly charged positive ions.[1–3] The method differs from conventional photoelectron spectroscopy in that the ionization is not direct. A ZEKE experiment consists of three phases. First, the sample is photoexcited by a pulsed light source to one or more ionization continua and/or pseudocontinua of high Rydberg states located near an ionization threshold. Second, unwanted photoelectrons produced with kinetic energy by direct ionization, fast autoionization, or both are removed during a chosen time delay that can last, depending on the system, from several hundreds of nanoseconds to several tens of microseconds. Third, at the end of this waiting phase, the high neutral Rydberg states that have remained in the excitation region are field ionized and extracted by a pulsed electric field, the magnitude and shape of which can be adjusted to achieve optimal resolution and sensitivity.[3–5] The first and third phases of a ZEKE experiment are reasonably well understood, but the rules that govern the evolution of the system during the second phase are only beginning to be unraveled. Those states that are optically accessible and initially populated in ZEKE spectroscopy are known, or estimated fairly accurately, but the nature of the states probed at the end of the delay time when the pulsed electric field is applied is unknown.

One surprising property of the states probed by delayed pulsed field ionization is their lifetime, which can exceed the lifetime of the optically accessible low-l, low-m_l (l and m_l refer to the orbital angular momentum and azimuthal quantum numbers, respectively) states by several orders of magnitude.[5–18] Several interpretations have been proposed for these lifetimes; some point at the importance of electric field and collisional effects[5,6,8–10,15] and others at intramolecular energy redistribution processes[7] and breakdown of the Born–Oppenheimer approximation.[11] We investigate in this paper how, under conditions typical for a ZEKE experiment, neighboring charged particles can induce l and m_l mixing in a high Rydberg state and thereby prolong the state's lifetime by spreading its wave function among nonpenetrating, stable high-l, high-m_l orbitals. This work complements recent investigations[5–18] and leads us to propose an interpretation of most experimental observations made to date concerning the lifetimes of the states probed by ZEKE photoelectron spectroscopy.

Chupka[5] was the first to point out that, for NO, the lifetime of the states probed in the ZEKE experiment[2,4,6] was too long for the optically accessible predissociative p series although possibly compatible with that of the f series. He further suggested that l mixing (or Stark mixing) induced by electric fields could prolong the lifetime by a factor of n (n is the Rydberg principal quantum number) by spreading the Rydberg wave function equally among all n states with l values from 0 to $n-1$. Indeed, high-l states do not penetrate into the core region and are stable against predissociation and autoionization. Similarly, collisional interactions with ions or neutrals could induce m_l mixing and increase the lifetime by an additional factor of n.[5] Pratt[6] then showed that relatively weak dc electric fields could lead to the almost complete disappearance of the ZEKE signal in NO, a phenomenon he attributed to field-induced predissociation. In experiments[9] in which the ZEKE spectrum of the Rydberg states located below the two spin–orbit states ($^2P_{3/2}$ and $^2P_{1/2}$) of Ar^+ was recorded, and the measured lifetimes compared with those obtained[19] from a line shape analysis of the optically accessible s' and d' series, the states probed by ZEKE spectroscopy (called "ZEKE" states below) were found to be unexpectedly long lived, and their lifetimes

 0021-9606/94/101(5)/3495/11/$6.00

could not be explained solely by the effects of homogeneous dc electric fields. Indeed, as for NO, dc electric fields of 2–3 V/cm were found to cause the disappearance of the ZEKE signals. Zhang, Smith, and Knee[8] demonstrated that the lifetime of the ZEKE states depended on the fluence of the ionizing lasers; high laser fluences shortened the lifetime of the highest Rydberg states, but the lifetime was independent of the pressure of the sample gas, a conclusion also reached by Bahatt, Even, and Levine.[7]

Three paradoxes are apparent in these observations. (1) Whereas dc electric fields undoubtedly contribute to enhance the lifetime of the ZEKE states in some systems, they also seem to cause the disappearance of the ZEKE signals in NO and Ar. Therefore, l mixing by electric fields cannot be the only source of, and can sometimes even shorten, the lifetimes of the ZEKE states. (2) How can collisional interactions, which also lead to l mixing, prolong lifetimes in cases in which electric fields fail to do so? (3) If collisional effects are the origin of the long lifetimes, why does an increase in the sample gas pressure not have any apparent effect on the lifetimes? One explanation of the first two paradoxes, based on experiments conducted under a wide range of pulsed and dc electric fields, proposes that for argon collisional l and m_l mixing alone can account for the observed lifetimes and that dc electric fields effectively *inhibit* the formation of the ZEKE states.[9] A major aim of this report is to investigate whether this suggestion can be substantiated by a simple calculation of collisional l and m_l mixing.

To model collisional interactions, we elaborate on Chupka's l and m_l mixing interpretation.[5] We adopt a perturbative approach and investigate whether an inhomogeneous, noncylindrically symmetrical electric field that consists of a homogeneous part (corresponding to a weak stray or intentionally applied dc electric field) and an inhomogeneous part (corresponding to the field of a resting ion) can induce collisional l and m_l mixing in a high Rydberg state. The results enable us to distinguish between different regimes of l and m_l mixing depending on the magnitude of the homogeneous dc component of the electric field and the density of the perturbing ions, and they support the conclusion[9] that dc electric fields can inhibit collisional m_l mixing.

II. GENERAL CONSIDERATIONS

The states probed by delayed pulsed field ionization in a ZEKE experiment have principal quantum numbers n that typically range from 100 to 250. Higher Rydberg states are difficult to observe in ZEKE experiments either because their large radius makes them very sensitive to collisional ionization or because the weak electric fields inevitably present in the ionization region are sufficient to ionize them. Indeed, the lowering of an ionization threshold (in cm^{-1}) by a homogeneous dc electric field of magnitude F (in V/cm) amounts to approximately $6F^{1/2}$. Table I lists the classical radius and energy of Rydberg states as a function of their principal quantum number n and the minimum dc field required for their field ionization.

Charged particles are usually produced near the high Rydberg states in ZEKE experiments. Their density depends on the experimental conditions (laser fluence, carrier gas, ionization scheme, etc.) and lies typically between 10 and 10^6 ions/mm^3. The distance between a Rydberg atom or molecule and the nearest ion may therefore vary between 1 μm and 1 mm; a typical distance is 50 μm. The field of an ion at a distance r from the point charge equals $Ze/(4\pi\epsilon_0 r^2)$ and is given in Table II for a series of values of r. Only Rydberg states with principal quantum number n smaller than the n values listed in Table II are stable in the presence of the electric field of the perturbing ion. Furthermore, the thermal velocity of the ions in the ionization region may range from 20 to 500 m/s depending on the expansion conditions. Such ions can travel up to 500 μm during a delay time of 1 μs. Too high a density of charged particles in the ionization region may therefore lead to the collisional ionization of all high Rydberg states before the pulsed electric field is applied and prevent the observation of a ZEKE signal. Although trivial, these considerations account for the observation made by Zhang, Smith, and Knee[8] that the highest Rydberg states are less likely to be detected by delayed pulsed field ionization with increasing laser fluence and/or delay time between photoexcitation and the pulsed electric field.

TABLE I. Classical radius and energy of a Rydberg state with principal quantum number n and magnitude of the minimum electric field required for its field ionization.

n	E_n−IP (cm^{-1})	E (V/cm)	r (μm)
50	−44	53	0.13
100	−10.9	3.3	0.53
150	−4.9	0.67	1.2
200	−2.7	0.21	2.1

The weak stray fields of the order of 20–100 mV/cm that are always present in ZEKE experiments[1–4,20–22] can induce a significant degree of Stark mixing (l mixing). Analogies exist between the high Rydberg states of most atoms and molecules and those of the hydrogen atom. Consequently, the hydrogenic Rydberg states form a good starting point for a discussion of the Stark effect in more complex systems. In the presence of a homogeneous electric field, l ceases to be a good quantum number. The states are more conveniently labeled with the parabolic quantum numbers n_1 and n_2, which can take on the values from 0 to $n-1$ and satisfy the condition $n_1+n_2+|m|+1=n$ (See Ref. 23 for more details). In the hydrogen atom, all $|l,m_l\rangle$ states (or equivalently all $|n_1,n_2m\rangle$ states) associated with a given value of n are de-

TABLE II. Electric field of an ion (in V/cm) at various distances r from the point charge. All Rydberg states with principal quantum number n equal to or higher than the values listed in the third column can be ionized by the electric field given in the second column.

r (μm)	E (V/cm)	n
0.1	1.44×10^3	22
1	14.4	70
5	0.576	155
10	0.144	220
100	1.44×10^{-3}	695
1000	1.44×10^{-5}	2200

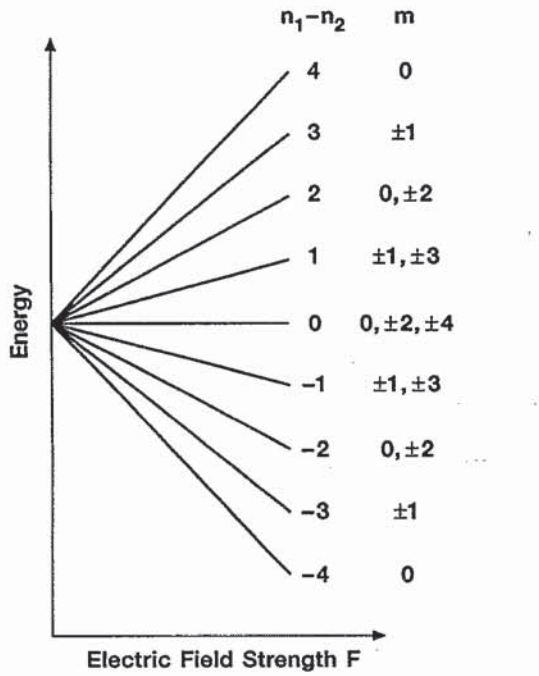

FIG. 1. Energy level structure (not to scale) of the Stark states in hydrogen.

generate in the absence of an electric field. In the presence of a homogeneous electric field of strength F, the Stark structure of a Rydberg state of hydrogen is given to second order by

$$E(n,n_1,n_2,m) = R_H[1-1/n^2+3(F/5.1422\times10^9)n(n_1-n_2) - 1/8(F/5.1422\times10^9)^2n^4(17n^2-3(n_1-n_2)^2 - 9m^2+19)], \quad (1)$$

where the factor 5.1422×10^9 converts atomic electric field units to V/cm. The first two terms in the square brackets on the right-hand side of Eq. (1) correspond to the Rydberg formula; the third and fourth terms represent the linear and quadratic Stark effects, respectively. At low to moderate field strengths, the energy level structure is fairly well characterized by the linear Stark effect. Figure 1 shows a schematic diagram of the Stark level structure of an $n=5$ Rydberg state of hydrogen. The situation can easily be generalized to higher values of n. Most levels, particularly those located in the middle of the Stark manifold, still display a large amount of m_l degeneracy.

In larger atoms and in molecules, the situation is more complex:[24–29] the high-l states, which have vanishing quantum defects, form a hydrogenic manifold of almost degenerate states at zero fields. In the presence of electric fields, these states behave rather similarly to the situation described above for hydrogen. Their energy level structure is dominated by the linear Stark effect. The low-l states that have nonzero quantum defects are separated from the high-l hydrogenic manifold and start displaying a quadratic Stark effect at low field strengths before they merge into and start interacting with the hydrogenic Stark manifold of high-l states at intermediate field strengths.[24,29] Although Eq. (1) is relatively accurate at low field strengths, it becomes invalid once the Stark manifolds that correspond to successive values of n overlap. Interactions between states that have the same azimuthal quantum number m but belong to different n lead to avoided crossings. These avoided crossings are particularly marked at low values of m and become increasingly widespread as the field strength increases.[24] As a result, the near degeneracy between the m sublevels of a given Stark state, which at low fields are split only by the quadratic Stark effect, is broken at larger fields, a fact of considerable importance for the discussion to follow. Although some aspects of the interactions between high Rydberg states and colliding ions and neutrals have been discussed in Ref. 29, we focus here on the factors that are critically important to the process of m_l mixing and that have not been addressed in the earlier work.

III. SIMPLE MODEL FOR ION-RYDBERG INTERACTIONS

Unlike l, the azimuthal quantum number m_l remains a constant of motion as long as the potential felt by the Rydberg states retains cylindrical symmetry. Homogeneous and cylindrically symmetric electric fields therefore do not induce m_l mixing. For instance, in the absence of dc electric fields, a perturbing particle at rest in a coordinate system fixed at the center of mass of the ionic core of a Rydberg atom or molecule cannot cause any m_l mixing, nor can a particle moving toward the Rydberg atom with vanishing impact parameter. A wide range of external perturbations could contribute to induce m_l mixing in a ZEKE experiment, e.g., a dc electric field and the field of a resting particle (ionic or neutral), a distribution of static charges, a magnetic field and an electric field not parallel to each other, a particle (ion, electron, or neutral) moving toward the Rydberg atom with nonzero impact parameter, or any combinations of these. Although all these perturbations may be significant, we consider here only the case of a Rydberg atom in a homogeneous electric field that is subject to the perturbation of a single ion located at a fixed distance R_I from the Rydberg center. This choice is justified because the ionization region in most ZEKE experiments is shielded to minimize magnetic fields. Also, the collisional effects were found to occur within a few tens of nanoseconds[6,9] and the distance traveled by all particles apart from electrons during this time is likely not to be sufficient to induce much m_l mixing. Finally if the collisional m_l mixing is induced by a distribution of charges, it is reasonable to begin by considering the effects of a single charged particle.

The situation is depicted in Fig. 2. The z axis is chosen to lie parallel to the electric field vector $\mathbf{F}$. The coordinate system is centered on the Rydberg atom. The polar coordinates of the Rydberg electron and of the perturbing ion in this system are labeled (r_e,θ_e,ϕ_e) and (R_I,θ_I,ϕ_I), respectively. The angle between the position vectors $\mathbf{R_I}$ and $\mathbf{r_e}$ is labeled θ_{Ie}. The starting point for the discussion is the Hamiltonian H for the hydrogen atom, which can be decomposed in three parts, the unperturbed Hamiltonian

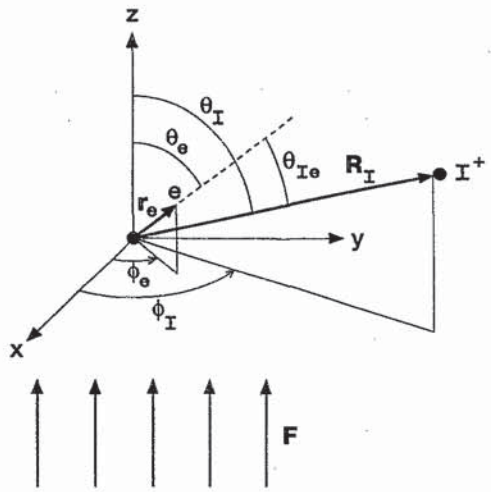

FIG. 2. Schematic representation of the model used to calculate m_l mixing in the high Rydberg states probed in ZEKE experiments. The coordinate system is centered on the Rydberg atom and the z axis is chosen to lie parallel to the electric field vector $\mathbf{F}$. The polar coordinates of the Rydberg electron and of the perturbing ion in this system are labeled (r_e,θ_e,ϕ_e) and (R_I,θ_I,ϕ_I), respectively. The angle between the position vectors $\mathbf{R_I}$ and $\mathbf{r_e}$ is labeled θ_{Ie}.

$$H_0=-\frac{\hbar^2}{2\mu}\nabla_e^2-\frac{e^2}{4\pi\epsilon_0 r_e},$$

the Stark operator $H_{\text{Stark}}=eFz$, and the perturbation V caused by the ion. The eigenproblem to be solved is then

$$H\Psi=(H_0+H_{\text{Stark}}+V)\Psi=E\Psi. \tag{2}$$

The form taken by the Stark operator eFz in polar and parabolic coordinates is found in the literature.[23–29]

The perturbation V of the Rydberg atom by the ion can be written as

$$V=\frac{e^2}{4\pi\epsilon_0}\left(\frac{1}{R_I}-\frac{1}{R_{Ie}}\right). \tag{3}$$

Because the position of the perturbing ion is considered fixed, the first term in Eq. (3) is constant and may be neglected. Using the expansion

$$\frac{1}{r_{12}}=\sum_{k=0}^{\infty}\frac{r_<^k}{r_>^{k+1}}P_k(\cos\theta), \tag{4}$$

where $r_<$ and $r_>$ stand, respectively, for the lesser and the greater of r_1 and r_2, θ for the angle between the position vectors $\mathbf{r_1}$ and $\mathbf{r_2}$, and $P_k(\cos\theta)$ is an ordinary Legendre polynomial, Eq. (3) can be rewritten as

$$V=-\frac{e^2}{4\pi\epsilon_0}\frac{1}{R_{Ie}}=-\frac{e^2}{4\pi\epsilon_0}\sum_{k=0}^{\infty}\frac{r_<^k}{r_>^{k+1}}P_k(\cos\theta_{Ie}). \tag{5}$$

The perturbing ion is assumed to lie sufficiently far from the Rydberg atom that R_I can be considered to a good approximation to be always greater than r_e. Applying the spherical harmonic addition theorem to Eq. (5) leads to

$$V(r_e,\theta_e,\phi_e,R_I,\theta_I,\phi_I)$$

$$=-\frac{e^2}{4\pi\epsilon_0}\sum_{k=0}^{\infty}\frac{r_e^k}{R_I^{k+1}}\frac{4\pi}{2k+1}$$

$$\times\sum_{q=-k}^{k}(-1)^q Y_{kq}(\theta_e,\phi_e)Y_{k-q}(\theta_I,\phi_I), \tag{6}$$

where the $Y_{lm}(\theta,\phi)$ represent spherical harmonics. Because the position of the perturbing ion is fixed, its coordinates R_I, θ_I, and ϕ_I enter Eq. (6) simply as parameters.

A solution to Eq. (2) can be sought either by treating V as a perturbation to a zero-order Stark Hamiltonian H_0+H_{Stark} or by treating $H_{\text{Stark}}+V$ as a perturbation to H_0. In the former case, the eigenfunctions of the unperturbed problem are Stark states which, as discussed above, are conveniently characterized in parabolic coordinates by the quantum numbers n, n_1, n_2, and m. The perturbation by the ion, though, has a simple form in spherical coordinates [see Eq. (6)] and the advantage of working in parabolic coordinates is largely lost. The parabolic eigenfunctions $|n,n_1,n_2,m\rangle$ can be represented as a linear combination of hydrogenic $|n,l,m_l\rangle$ functions

$$|n,n_1,n_2,m\rangle=\sum_l c_l|n,l,m_l\rangle$$

$$=\sum_l c_l R_{n,l}(r_e)Y_{lm}(\theta_e,\phi_e). \tag{7}$$

Considering interactions between levels that have the same n value only, the off-diagonal matrix elements of the perturbed system can be written as

$$\langle n,n_1,n_2,m|V|n,n_1',n_2',m'\rangle$$

$$=-\frac{e^2}{4\pi\epsilon_0}\sum_l c_l\sum_{l'} d_{l'}\sum_{k=0}^{\infty}\frac{1}{R_I^{k+1}}\frac{4\pi}{2k+1}$$

$$\times\int_{r_e=0}^{R}r_e^2 dr_e R_{n,l}(r_e)r_e^k R_{n,l'}(r_e)$$

$$\times\sum_{q=-k}^{k}(-1)^q\langle Y_{lm}|Y_{kq}|Y_{l'm'}\rangle Y_{k-q}(\theta_I,\phi_I), \tag{8}$$

where R is chosen to be sufficiently large that the integral over r_e has converged. Using standard angular momentum algebra,[30] Eq. (8) can be recast as

$$\langle n,n_1,n_2,m|V|n,n_1',n_2',m'\rangle=-\frac{e^2}{4\pi\epsilon_0}\sum_l c_l\sum_{l'} d_{l'}\sum_{k=0}^{\infty}\frac{1}{R_I^{k+1}}\frac{4\pi}{2k+1}\int_{r_e=0}^{R} r_e^2 dr_e R_{n,l}(r_e)r_e^k R_{n,l'}(r_e)$$
$$\times\sum_{q=-k}^{k}(-1)^{q+m}\sqrt{\frac{(2l'+1)(2k+1)(2l+1)}{4\pi}}\begin{pmatrix} l' & k & l \\ m' & q & -m\end{pmatrix}$$
$$\times\begin{pmatrix} l' & k & l \\ 0 & 0 & 0\end{pmatrix}Y_{k-q}(\theta_I,\phi_I). \tag{9}$$

In the case in which the Hamiltonian is set up in the spherical basis with the perturbation $H_{\text{Stark}}+V$, the matrix elements of V are simply

$$\langle n,l,m|V|n,l',m'\rangle=-\frac{e^2}{4\pi\epsilon_0}\sum_{k=0}^{\infty}\frac{1}{R_I^{k+1}}\frac{4\pi}{2k+1}\int_{r_e=0}^{R} r_e^2 dr_e R_{n,l}(r_e)r_e^k R_{n,l'}(r_e)$$
$$\times\sum_{q=-k}^{k}(-1)^{q+m}\sqrt{\frac{(2l'+1)(2k+1)(2l+1)}{4\pi}}\begin{pmatrix} l' & k & l \\ m' & q & -m\end{pmatrix}\begin{pmatrix} l' & k & l \\ 0 & 0 & 0\end{pmatrix}Y_{k-q}(\theta_I,\phi_I). \tag{10}$$

Some simple conclusions can be drawn from Eqs. (9) and (10); first, the number of nonvanishing terms is determined by the convergence of the expansion (4), which in turn depends on the value of R_I. In addition, the nonvanishing terms must fulfill the conditions

$$m'=m-q \quad \text{with} \quad -k\leqslant q\leqslant k, \tag{11a}$$

and

$$l'=l,l\pm 1,\ldots,l\pm k. \tag{11b}$$

The perturbation by the electric field of the ion therefore mixes l as well as m_l. Finally from the relation

$$Y_{lm}(0,\phi)=\sqrt{\frac{2l+1}{4\pi}}\,\delta_{m0} \tag{12}$$

it follows, as expected, that no m_l mixing occurs when $\theta_I=0$, i.e., when the perturbing ion lies along the z axis and the total electric field perturbing the Rydberg atom is cylindrically symmetric. The term with $k=0$ in Eq. (10) leads to a constant energy shift of $-e^2/(4\pi\epsilon_0 R_I)$ of all diagonal elements and exactly counterbalances the first (neglected) term in Eq. (3). To evaluate the radial integral in Eqs. (9) and (10), we use Eq. (13), which was obtained by generalizing to any non-negative integer value of k, and to cases in which l differs from l', the procedure used in Ref. 23 to derive Eqs. 3.20 to 3.23. We find

$$\int_{r_e=0}^{R} r_e^2 dr_e R_{n,l}(r_e)r_e^k R_{n,l'}(r_e)=\left(\frac{na_0}{2Z}\right)^k\frac{\sqrt{(n-l-1)!(n-l'-1)!}}{2n\sqrt{(n+l)!(n+l')!}}(-1)^{n+l'}(k+2+l+l')!$$
$$\times\sum_{\alpha=0}^{n-l-1}(-1)^{\alpha}\begin{pmatrix} k+2+l+l'+\alpha \\ \alpha\end{pmatrix}\begin{pmatrix} n+l \\ 2l+1+\alpha\end{pmatrix}$$
$$\times\sum_{\gamma=0}^{2l'+1}(-1)^{\gamma}\begin{pmatrix} 2l'+1 \\ \gamma\end{pmatrix}\begin{pmatrix} k+1-l'+l+\alpha+\gamma \\ n+l'\end{pmatrix}, \tag{13}$$

where a_0 represents the Bohr radius.

In either case outlined above, the evaluation of the extent of l and m_l mixing, even if only interactions between levels of the same principal quantum number n are considered, requires the diagonalization of an $n^2\times n^2$ matrix, which, for the high n states probed by ZEKE spectroscopy, leads to a prohibitively large computation. Moreover, given the small spacing between successive n terms, which scales as $2R_H/n^3$, a calculation must include several n values to be accurate. The goal of this report is not to give a quantitative description of the physical situation but rather to investigate qualitatively at which values of R_I, m_l mixing is expected to be significant. Thus, instead of attempting to solve Eq. (2) by diagonalizing the $n^2\times n^2$ Hamiltonian for $n\geqslant 100$, which, in the spherical basis, takes the form (with H^s referring to H_{Stark})

$$
H=\begin{vmatrix}
|0,0\rangle & |1,-1\rangle & |1,0\rangle & |1,1\rangle & |2,-2\rangle & |2,-1\rangle & |2,0\rangle & |2,1\rangle & |2,2\rangle & \cdot & |n-1,n-1\rangle \\
E_0 & V_{0,0}^{1,-1} & H_{0,0}^{s1,0}+V_{0,0}^{1,0} & V_{0,0}^{1,1} & V_{0,0}^{2,-2} & V_{0,0}^{2,-1} & V_{0,0}^{2,0} & V_{0,0}^{2,1} & V_{0,0}^{2,2} & \cdot & V_{0,0}^{n-1,n-1} \\
 & E_1 & V_{1,-1}^{1,0} & V_{1,-1}^{1,1} & V_{1,-1}^{2,-2} & H_{1,-1}^{s2,-1}+V_{1,-1}^{2,-1} & V_{1,-1}^{2,0} & V_{1,-1}^{2,1} & V_{1,-1}^{2,2} & \cdot & V_{1,-1}^{n-1,n-1} \\
 & & E_1 & V_{1,0}^{1,1} & V_{1,0}^{2,-2} & V_{1,0}^{2,-1} & H_{1,0}^{s2,0}+V_{1,0}^{2,0} & V_{1,0}^{2,1} & V_{1,0}^{2,2} & \cdot & V_{1,0}^{n-1,n-1} \\
 & & & E_1 & V_{1,1}^{2,-2} & V_{1,1}^{2,-1} & V_{1,1}^{2,0} & H_{1,1}^{s2,1}+V_{1,1}^{2,1} & V_{1,1}^{2,2} & \cdot & V_{1,1}^{n-1,n-1} \\
 & & & & E_2 & V_{2,-2}^{2,-1} & V_{2,-2}^{2,0} & V_{2,-2}^{2,1} & V_{2,-2}^{2,2} & \cdot & V_{2,-2}^{n-1,n-1} \\
 & & & & & E_2 & V_{2,-1}^{2,0} & V_{2,-1}^{2,1} & V_{2,-1}^{2,2} & \cdot & V_{2,-1}^{n-1,n-1} \\
 & & & & & & E_2 & V_{2,0}^{2,1} & V_{2,0}^{2,2} & \cdot & V_{2,0}^{n-1,n-1} \\
 & & & & & & & E_2 & V_{2,1}^{2,2} & \cdot & V_{2,1}^{n-1,n-1} \\
 & & & & & & & & E_2 & \cdot & V_{2,2}^{n-1,n-1} \\
 & & & & & & & & & \cdot & \cdot \\
 & & & & & & & & & & E_{n-1}
\end{vmatrix} \tag{14}
$$

we follow two different simplifying approaches. We consider first m_l mixing by the perturbation V at a single value of l. The extent of m_l mixing is obtained, in this simple calculation, by diagonalizing the matrix

$$
\begin{vmatrix}
|l-l\rangle & |l-l+1\rangle & |l-l+2\rangle & \cdot & \cdot & |ll\rangle \\
E_{l,l} & V_{l,-l}^{l,-l+1} & V_{l,-l}^{l,-l+2} & \cdot & \cdot & V_{l,-l}^{ll} \\
 & E_{l,-l+1} & V_{l,-l+1}^{l,-l+2} & \cdot & \cdot & V_{l,-l+1}^{ll} \\
 & & E_{l,-l+2} & \cdot & \cdot & V_{l,-l+2}^{ll} \\
 & & & \cdot & \cdot & \cdot \\
 & & & \cdot & \cdot & \cdot \\
 & & & & & E_{l,l}
\end{vmatrix} . \tag{15}
$$

Clearly this procedure is equivalent to neglecting all matrix elements that connect the l block considered with other l blocks in Eq. (14), in particular the elements of the Stark operator that connect blocks with $l'=l\pm1$. This neglect can be partially compensated for by making some assumptions concerning the values of the diagonal elements; in other words, by considering the matrix as "prediagonalized." A prediagonalization, however, necessarily causes an alteration of the basis functions. This calculation therefore cannot be expected to be highly accurate but only to give rough guidelines.

If the diagonal elements in matrix (14) were chosen to be degenerate, as for a vanishing dc electric field F, any nonzero values for the elements of the perturbation matrix V would lead to extensive m_l mixing. Such a result, however, is not physically meaningful. Indeed, in this case, the electric field perturbing the Rydberg atom is still cylindrically symmetrical. This artefact comes from the fact that one direction in space has been singled out as z axis (see Fig. 2), although there are no reasons to do so in the absence of an electric field. To avoid such an artefact, only cases in which the hierarchy $H_{\text{Stark}}>V$ is obeyed are considered, i.e., cases in which the main features of the energy spectrum are determined by $H+H_{\text{Stark}}$. This condition is automatically obeyed at distances R_I large enough for the field of the ion to be less in magnitude than the homogeneous dc field.

As explained in Sec. II, a fair amount of m_l degeneracy remains in the hydrogen atom at low electric fields (see Fig. 1); indeed, at a given value of n_1-n_2 the m_l sublevels are split only by the quadratic Stark effect [Eq. (1)]. We begin by considering how the perturbation mixes these nearly degenerate states. We calculate the extent of m_l mixing induced by a perturbing ion located at a distance R_I by finding and squaring the eigenvectors of matrix (15) and performing a spatial average over θ_I and ϕ_I. To retain some of the characteristics of the hydrogenic case (see Fig. 1), we keep only even m_l values. Figure 3 illustrates the results obtained for the $l=30$ block of the $n=100$ state with the assumption that the diagonal elements prior to diagonalization are split by the quadratic Stark effect as given by Eq. (1) for a field of 100 mV/cm. Substantial m_l mixing occurs already at $R_I=200$ μm, a distance at which the field of the ion is only 3.6×10^{-4} V/cm. Figure 4, on the other hand, illustrates the situation in which the $m_l=0$ state is separated from the rest of the m_l manifold by the distance that separates two adjacent members of the Stark manifold [i.e., by $3R_{\text{H}}nF$ (in V/cm)/5.1422×10^9 cm^{-1}]. In this case, the extent of m_l mixing is still negligible at $R_I=25$ μm and begins to be noticeable at $R_I=15$ μm.

The second approach followed to solve Eq. (2), without having to diagonalize prohibitively large matrices or restrict the treatment to a single l block, consists of finding the eigenvectors of matrix (14) at relatively small values of n and scaling the perturbations V and H_{Stark} so as to have conditions that approximate the situation for high n values. A simple and approximate approach to this scaling is to ensure that the off-diagonal matrix elements of V and H_{Stark} have the same magnitude regardless of the value of n. For the Stark perturbation, this scaling can be achieved by adapting the value of the electric field to the value of n. Scaling the perturbation caused by the ion is more problematic; successive terms in expansion (6) ought to be scaled differently as they contain different powers of k. An approximate scaling can be made, however, by adapting the value of R_I so that

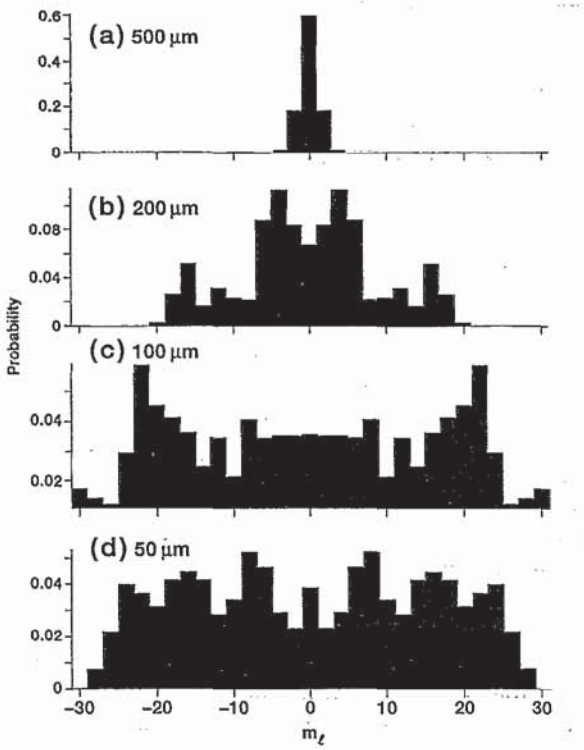

FIG. 3. The m_l mixing induced by a singly charged ion for an $n=100$, $l=30$ Rydberg state. The m_l levels are assumed to be split in zero order by the quadratic Stark effect at a field of 100 mV/cm. The figure illustrates how the $m_l=0$ state gradually becomes mixed with other m_l states as the distance between the Rydberg atom and the perturbing ion is reduced from 500 μm (a) to 50 μm (d).

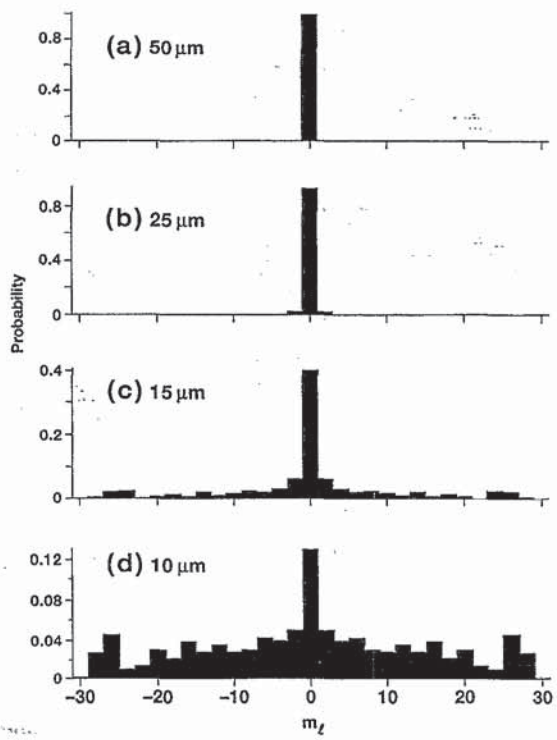

FIG. 4. The m_l mixing induced by a singly charged ion for an $n=100$, $l=30$ Rydberg state. The $m_l=0$ state is assumed to be separated from the rest of the m_l manifold by the energy separating two adjacent members of the Stark manifold at a field of 100 mV/cm. The figure illustrates how the $m_l=0$ state gradually becomes mixed with other m_l states as the distance between the Rydberg atom and the perturbing ion is reduced from 50 μm (a) to 10 μm (d).

the terms with $k=1$, which are by far the largest of all l and m_l mixing terms, remain constant with n. Both the $k=1$ terms of the V operator and the Stark perturbation eFz are proportional to the integral $\int_{r_e=0}^{R} r_e^2 dr_e R_{n,l}(r_e) r_e R_{n,l'}(r_e)$, which scales as $n(n^2-l^2)^{1/2}$. For low to intermediate values of l, this integral scales as n^2, whereas in the limit at which $l=n-1$ it scales as $n^{3/2}$. For $m=l=n-1$, the Stark perturbation scales as n. An $n=100$ Rydberg state that is in a field of 100 mV/cm and is at a distance of 50 μm from the perturbing ion could be represented by an $n=14$ Rydberg state in the presence of either a field of 5.1 V/cm and an ion at 7 μm (scaling appropriate for the low-l situation) or by a field of 0.7 V/cm and an ion at 18 μm (scaling appropriate for the high-l, high-m_l limit). In the former case, the larger electric field results in a smaller degree of collisional l and m_l mixing than in the latter case, whereas the shorter distance to the ion leads to a larger degree of collisional l and m_l mixing; both effects act in opposite directions.

Figures 5–7 demonstrate the effect of m_l mixing induced in representative components of the Stark manifold by an ion located at several distances from an $n=14$ Rydberg atom in a field of 5.1 V/cm. As before, m_l mixing is evaluated by squaring the eigenvectors and averaging over θ_l and ϕ_l. The histogram bars represent the probability of a given state to be found in a given $|l,m_l\rangle$ basis function. The abscissa is ordered by blocks of increasing l values, and by increasing m_l value within a given l block. Figure 5 illustrates m_l mixing in the $|0,0\rangle$ zero-order state, which correlates at large distance R_I to the nondegenerate $|n_1=n-1,n_2=0,m=0\rangle$ Stark state (the highest energy state in the Stark manifold). The m_l mixing is negligible at 5 μm and begins at around 2.5 μm. Figure 6 displays the situation that occurs for the $|6,0\rangle$ zero-order state, which correlates at large distances R_I to the

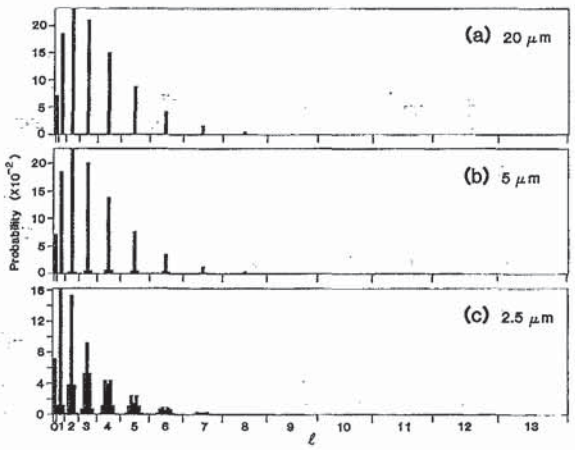

FIG. 5. The m_l mixing in the $|n=14,l=0,m_l=0\rangle$ zero-order state, which correlates, at large distance R_I, to the nondegenerate $|n_1=13,n_2=0,m=0\rangle$ Stark state (the highest energy state in the Stark manifold). (a) $R_I=20$ μm, (b) $R_I=5$ μm, (c) $R_I=2.5$ μm.

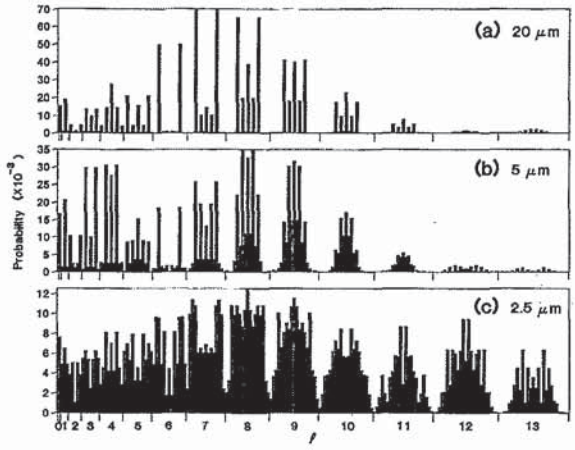

FIG. 6. The m_l mixing in the $|n=14,l=6,m_l=0\rangle$ zero-order state, which correlates, at large distance R_I, to the $|n_1=2,n_2=11,m=0\rangle$ Stark state [which belongs to the fivefold degenerate Stark level with $(n_1-n_2)=-9$ and $m=0,\pm2,\pm4$]. (a) $R_I=20$ μm, (b) $R_I=5$ μm, (c) $R_I=2.5$ μm.

fivefold degenerate Stark state with $n_1=2$, $n_2=11$ and $m=0$. This state is degenerate with four other states of the same n_1-n_2 value but with m values of -4, -2, $+2$, and $+4$, respectively. At an ion distance of 20 μm a significant amount of m_l mixing has already taken place but only among states with $m_l=-4$, -2, 0, 2, and 4. The mixing is primarily caused by interactions between the degenerate Stark levels. At 5 μm, mixing between states of different n_1-n_2 becomes significant and mixing with $m_l=\pm1$, ±3, and to a lesser extent ±5, is apparent. At 2.5 μm, the mixing is extensive among all states with $m_l<11$ but the highest m_l states have not mixed in yet. At 20 μm from the ion, m_l mixing in the $|13,0\rangle$ state, which correlates at large distances R_I to the $n_1=6$, $n_2=7$, and $m=0$ Stark state, is already extensive, as can be seen in Fig. 7. This state is degenerate with 12 other levels with $m=\pm2$, ±4, ±6, ±8, ±10, and ±12. At this distance, the ion induces a negligible amount of mixing among neighboring members of the Stark manifold, as can be seen from the vanishing contribution in Fig. 7(a) of odd m_l values.

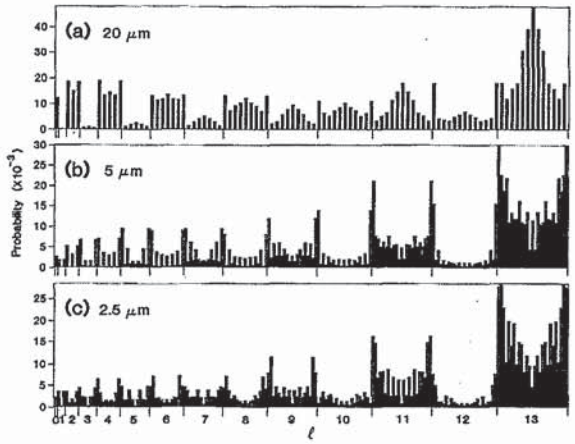

FIG. 7. The m_l mixing in the $|n=14,l=13,m_l=0\rangle$ zero-order state, which correlates, at large distance R_I, to the $|n_1=6,n_2=7,m=0\rangle$ Stark state (which belongs to the 13-fold degenerate Stark level with $(n_1-n_2)=-1$ and $m=0,\pm2,\ldots,\pm12$). (a) $R_I=20$ μm, (b) $R_I=5$ μm, (c) $R_I=2.5$ μm.

The onset of m_l mixing in an $n=100$ Rydberg state can be extrapolated from Figs. 4–7 by scaling R_I. The scaling factor for R_I lies between 7.1 (low-l limit) and 2.6 (high-l limit). Mixing among degenerate members of the Stark manifold (i.e., among states with the same n_1-n_2 value) is expected to be extensive at distances R_I as large as 150 (50) μm. The onset of mixing between states of different n_1-n_2 value is predicted at 18 (7) μm. These values are within a factor of 2 of the values predicted by the first approach (see Figs. 3 and 4). Figures 5–7 also reveal that collisional l and m_l mixing, although extensive under some conditions, is rarely uniform among all $|l,m_l\rangle$ states. The agreement between these two different approaches encourages us to believe that these calculations have captured the essential behavior of high Rydberg states in the presence of an ion.

The collisional l and m_l mixing process described above, however, will not be of any significance in ZEKE spectroscopy unless its time scale is shorter than 1 μs, the typical time delay between photoexcitation and pulsed field ionization. A rough estimate for this time scale can be obtained for high n values from the Fermi–Wentzel golden rule

$$\Gamma=2\pi\rho_{l,m_l>2}(V_{l,m_l<2,l',m_{l'}>2})^2, \tag{16}$$

where Γ and ρ stand for the decay rate of the initially prepared state and for the density of long-lived dark states, respectively. The off-diagonal matrix elements of V with $k=1$ equals approximately 2×10^{-4} cm^{-1} at a distance of $R_I=20$ μm and 0.3×10^{-4} cm^{-1} at a distance of $R_I=50$ μm. For the high-n states probed in ZEKE experiments, the density ρ of dark states coupled to a specific $|l,m_l\rangle$ amounts to between n and n^2 states in an energy width (in cm^{-1}) given by the spread of the Stark manifold $[6R_Hn^2(F/5.1422\times10^9)]$. Evaluation of Eq. (16) for $n=100$, $F=0.1$ V/cm, and $R_I=50$ μm leads to a mixing time scale of less than 0.1 μs.

Because the quantum numbers l and m_l are conjugate variables to the angles θ and ϕ, respectively, the mixing of l and m_l discussed in this paper is accompanied by an angular localization of the Rydberg wave function. This effect is illustrated in Figs. 8(a)–8(d). The electron density in the xz plane (See Fig. 2 for the definition of the axes) of the $|n=14,l=13,m=0\rangle$ Rydberg orbital can be seen in Fig. 8(a). It is very weak in the ion core region, as expected for a nonpenetrating orbital, and also symmetrical with respect to reflection through the xy, xz, and yz planes. Figures 8(b) and 8(c) show the electron density of the $|n=14,n_1-n_2=-1,m=0\rangle$ and $|n=14,n_1-n_2=13,m=0\rangle$ Stark states ($F=5.1$ V/cm), respectively. In both cases, the electron density is displaced along the z axis, and l mixing causes, as anticipated, a certain degree of constraint in the possible values of the angle θ. Since the energy of the $|n=14,n_1-n_2=-1,m=0\rangle$ is lowered slightly in the presence of the electric field (See Fig. 1), the electron density is shifted along the $-z$ axis. On the other hand, the $|n=14,n_1-n_2=13,m=0\rangle$ state is the highest energy state in the Stark manifold and the electric field displaces the electron density markedly in the $+z$ direction. The electron den-

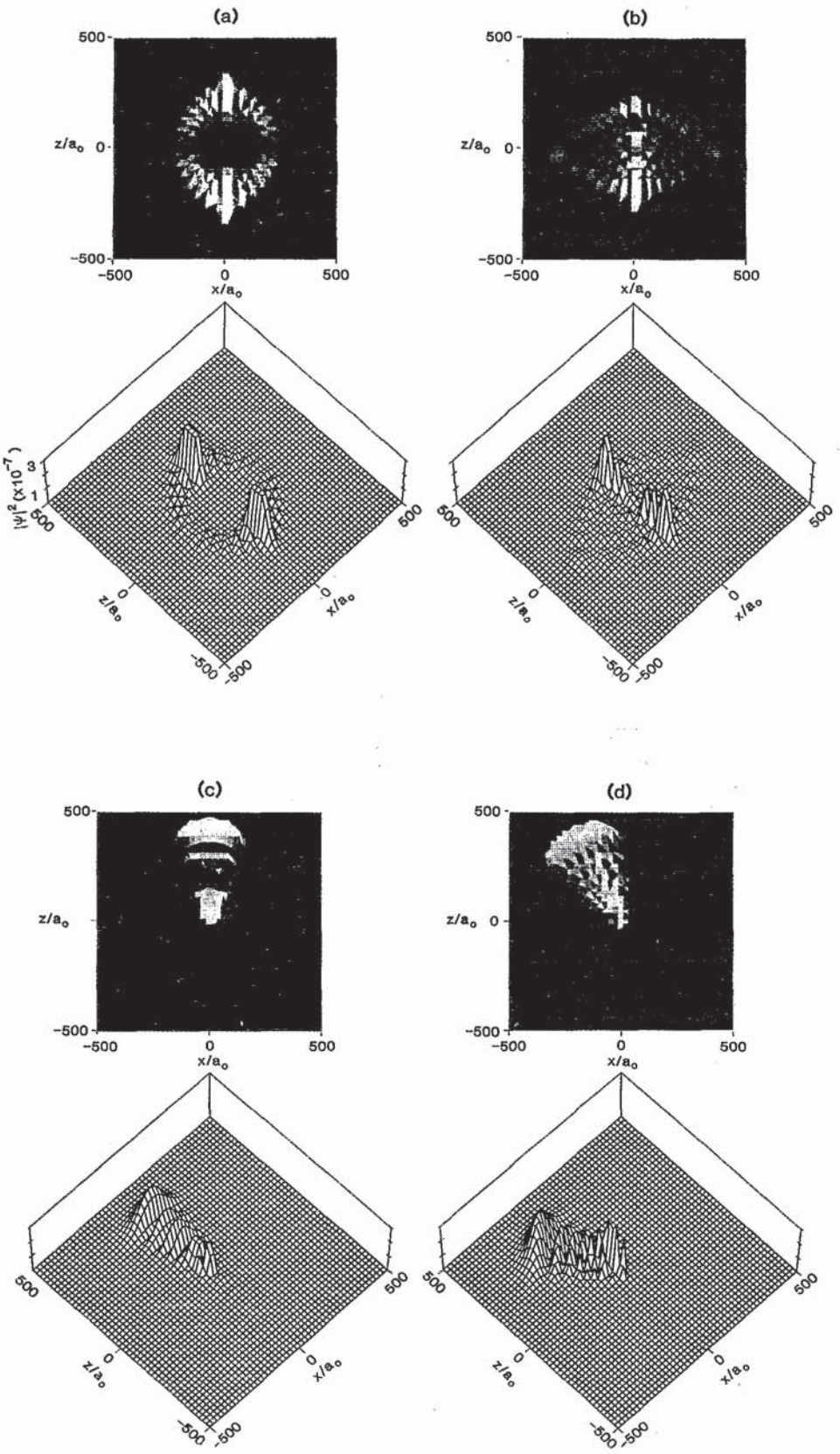

FIG. 8. Electron density of (a) the $|n=14,l=13,m=0\rangle$ Rydberg orbital, (b) the $|n=14,n_1-n_2=-1,m=0\rangle$ Stark state in the presence of an electric field $F=5.1$ V/cm, (c) the $|n=14,n_1-n_2=13,m=0\rangle$ Stark state in the presence of an electric field $F=5.1$ V/cm, and (d) the m_l mixed state that correlates at large distances R_l to the $|n_1-n_2=13,m=0\rangle$ Stark state. The perturbing ion is located in the xz plane ($\phi_l=0$ and $\theta_l=3\pi/8$ in Fig. 2) and at 2.5 μm from the Rydberg core in the presence of an electric field of 5.1 V/cm. In each case, the upper panel represents an aerial view of the lower panel.

sity of both states is still cylindrically symmetrical around the z axis and no preference exists for any specific value of the angle ϕ. The constraint in the possible values of ϕ that results from m_l mixing by an ion can be seen in Fig. 8(d). This figure illustrates how the electron density loses its cylindrical symmetry around the z axis and starts displaying a certain degree of angular localization. The state whose electron density is represented in Fig. 8(d) correlates at large distances R_I to the $|n_1-n_2=13,m=0\rangle$ Stark state, and the perturbing ion is located in the xz plane ($\phi_I=0$ and $\theta_I=3\pi/8$ in Fig. 2) and at 2.5 μm from the Rydberg core. The localization of the electron density, which is apparent in Fig. 8(d), can also be viewed as the formation of a molecular orbital. Whether the electron density of a l and m_l mixed state is shifted toward or from the perturbing ion depends on whether this orbital has bonding or antibonding character. Based on these considerations, we conclude that the electrons probed by pulsed field ionization in ZEKE spectroscopy often are shared by two or more ionic cores.

IV. DISCUSSION AND CONCLUSIONS

Before discussing the results predicted by the model presented above, we recapitulate its main features. We follow Chupka's interpretation that the long lifetime of the ZEKE states is a consequence of field-induced and collisional l and m_l mixing in high Rydberg states.[5] The nature of the states probed in a ZEKE experiment can be influenced by a number of external perturbations: weak stray (or intentionally applied) dc fields, ionic and neutral perturbers, magnetic fields, etc. The long-range nature of the Coulomb potential renders ions a likely source of l and m_l mixing collisional interactions. To model these interactions, we therefore consider the somewhat idealized situation that these external perturbations can be approximated by the effect of an inhomogeneous electric field that consists of a homogeneous dc component and an inhomogeneous component that corresponds to the field of a static ion. Several factors justify this simplification: first, collisional interactions appear to occur within a few tens of nanoseconds,[6,9] a time during which the motion of ions is negligible. Second, if collisional l and m_l mixing is caused by a distribution of ions rather than by a single ion, the main contribution will be that of a single ion, namely the ion lying closest to the Rydberg system.

To avoid the diagonalization of prohibitively large matrices (of dimension $n^2\times n^2$ when only one value of n is retained), we make additional simplifications that allow us to considerably reduce the dimension of the problem. The approximate nature of the model described above, and the approximations made within this model, rule out a quantitative evaluation of collisional l and m_l mixing in ZEKE experiments. Nevertheless, some qualitative features of the behavior (including lifetimes) of the high Rydberg states of hydrogen and more complex atoms and molecules probed in ZEKE experiments have been determined. In particular, the nature of the Rydberg wave function is greatly distorted from that of an unperturbed atom. As l and m_l mixing gains in importance, the wave function becomes localized in space and begins to form bonding or antibonding molecular orbitals with respect to two or more ion centers. We begin by summarizing the conclusions reached for hydrogen and then consider to what extent they also apply to nonhydrogenic Rydberg states.

A. Hydrogen

From the results of the simple calculations presented in the previous section, some limiting cases of l and m_l mixing can be defined depending on the experimental conditions. Different lifetime-prolonging factors (denoted c_τ below) can be estimated for each of these limiting cases. We assume that only the states with $l\leqslant 2$ are short lived, all others being metastable, and evaluate c_τ as the ratio of long-lived to short-lived character in a given mixed state.

(1) In the absence of perturbing ions, but in the presence of a homogeneous electric field, Stark mixing occurs but m_l mixing does not. In the limit at which the wave function is spread equally among all l states, the lifetimes are prolonged by a factor of $c_\tau=n/3$.

(2) At low ion densities (1–1000 ions/mm^3), m_l mixing arises only from interactions among near degenerate magnetic sublevels of a Stark level (characterized by its n_1-n_2 value). It therefore varies across the Stark profile, and becomes increasingly important as the center of the Stark manifold is approached, i.e., as the value of $|n_1-n_2|$ approaches 0. The lifetime is therefore dependent on the value of $|n_1-n_2|$. c_τ ranges from $n/3$ for Stark states located at the extremes of the Stark manifold to $c_\tau=(n/3)(n/6)=n^2/18$ (see Figs. 1,4–7) for the Stark sublevels with $n_1-n_2=0$. Owing to the larger statistical factor of the $n_1-n_2=0$ level, the lifetime will be prolonged by a factor closer to $n^2/18$ than to $n/3$.

(3) At higher ion densities ($>5\times10^4$ ions/mm^3), mixing occurs within all states of the Stark manifold, although the distribution among all $|l,m_l\rangle$ basis states is not expected to be uniform (Fig. 7). In the limit at which this distribution becomes uniform, the lifetimes are prolonged by a factor of $c_\tau=(n/3)^2=n^2/9$.

(4) At too high densities, collisional ionization of the Rydberg states becomes important and the lifetimes are shortened.

B. Other atoms and molecules

The Rydberg spectra of nonhydrogenic atoms[24–26,29] and molecules[27,28] differ from the hydrogenic case by the fact that, in general, the Rydberg series that correspond to low l values have nonzero quantum defects and are well separated, at low fields, from the hydrogenic manifold of high-l states. These low-l states correspond to the optically accessible states. At electric field strengths not sufficient to mix these low-l (and therefore low-m_l) states with the high-l manifold, the absorption cross section to the high-l manifold is negligible and no prolongation of the lifetimes occurs, either through Stark mixing or collisional m_l mixing. Nevertheless, the weak stray fields of typically 100 mV/cm present in ZEKE experiments are sufficient to mix the optically accessible low-l states with the hydrogenic high-l manifold and to induce an appreciable transition intensity to the high-l manifold.

This behavior can be demonstrated as follows. The high-l manifold starts to interact with a low-l state that has a nonzero quantum defect δ at field strengths for which the width of the Stark manifold of high-l states $[\approx 3R_H n^2(F/5.142\times10^9)]$ matches the energy separation with the low-l state $(2R_H\delta/n^3)$, i.e., at fields $F \geq 5.142\times10^9\,\delta/(3n^5)$. In the most unfavorable situation $\delta=0.5$, this field is 86 mV/cm for $n=100$. A significant part of the absorption cross section is therefore expected to go to the hydrogenic high-l manifold. Bordas and Helm[28] estimated that for the $n=70$ Rydberg state of H_3, approximately 83% of the intensity appears in the high-l manifold at a field strength of 100 mV/cm. The conclusions reached above for hydrogen are therefore also expected to apply to other nonhydrogenic systems at field strengths that correspond to typical stray fields in ZEKE experiments.

At larger field strengths than those typical for ZEKE experiments (i.e., at field strengths of more than 1 V/cm), nonhydrogenic systems display a different behavior from hydrogen. Indeed, as the field strength increases, Stark manifolds that correspond to adjacent values of n begin to interact, and the structure of the Stark spectrum is dominated by avoided crossings that are particularly important at low values of m_l.[24,29] As a result of these avoided crossings, the degeneracy between the optically accessible $m_l=0$ and 1 levels is lifted and mixing of these low-m_l states with higher m_l states is hindered. c_τ is reduced to $n/3$. Too large a dc field (of the order of 1 V/cm and greater) therefore can start inhibiting collisional l mixing, a conclusion which confirms the observation made in the study of the ZEKE spectrum of Ar[9] and NO.[6] In these systems, the role of the electric field is twofold: first, by inducing l mixing, it can enhance the decay rate of the initially prepared states by coupling them to more reactive autoionization (in the case of Ar) or predissociation (in the case of NO) channels. Second, by removing the near degeneracy of the magnetic sublevels of the Stark states, the electric field can inhibit m_l mixing and hence prevent the stabilization of the initially prepared states. Both effects contribute to the disappearance of the ZEKE signals observed in these systems.[6,9]

A new generation of PFI-ZEKE experiments[14,31,32] uses magnetic bottle photoelectron spectrometers to collect electrons. In these systems strong magnetic field are present. At a magnetic field strength of 1000 G or more, the motional or Lorentz electric field felt by the moving particles amounts to 1 V/cm or more depending on the gas expansion conditions. Although the magnetic field can contribute to induce m_l mixing, the calculations presented in this report suggest that the Lorentz electric field could also reduce ZEKE signals. These calculations are also expected to have important consequences for the technique of mass-analyzed threshold ionization (MATI) spectroscopy,[33] as this method relies on relatively large dc electric fields to eliminate unwanted ions. In this case, the reduction of the MATI signal can be avoided by using two pulsed electric fields as demonstrated in Ref. 34. The model described in this report is successful in explaining seemingly contradicting observations and contributes to our understanding of the complicated physical phenomena at play in ZEKE photoelectron spectroscopy. Such a step is important for the interpretation of results and the design of new experiments.

ACKNOWLEDGMENTS

We thank Hao Xu, Neil Shafer, Hongkun Park, and many other workers in this field for their comments. F.M. gratefully acknowledges the financial support of the Fond National Suisse de la Recherche Scientifique. This work was supported in part by the U.S. National Science Foundation under Grant Nos. NSF CHE 89-21198 and NSF CHE 93-22690.

[1] K. Müller-Dethlefs, M. Sander, and E. W. Schlag, Chem. Phys. Lett. **112**, 291 (1984).
[2] K. Müller-Dethlefs and E. W. Schlag, Annu. Rev. Phys. Chem. **42**, 109 (1991), and references therein.
[3] F. Merkt and T. P. Softley, Int. Rev. Phys. Chem. **12**, 205 (1993), and references therein.
[4] G. Reiser, W. Habenicht, K. Müller-Dethlefs, and E. W. Schlag, Chem. Phys. Lett. **152**, 119 (1988).
[5] W. A. Chupka, J. Chem. Phys. **98**, 4520 (1993).
[6] S. T. Pratt, J. Chem. Phys. **98**, 9241 (1993).
[7] D. Bahatt, U. Even, and R. D. Levine, J. Chem. Phys. **98**, 1744 (1993).
[8] X. Zhang, J. M. Smith, and J. L. Knee, J. Chem. Phys. **99**, 3133 (1993).
[9] F. Merkt, J. Chem. Phys. **100**, 2623 (1994).
[10] W. A. Chupka, J. Chem. Phys. **99**, 5800 (1993).
[11] U. Even, M. Ben-Nun, and R. D. Levine, Chem. Phys. Lett. **99**, 5800 (1993).
[12] W. G. Scherzer, H. L. Selzle, and E. W. Schlag, Z. Naturforsch. Teil A **48**, 1256 (1993).
[13] W. A. Chupka, Abstracts, European Research Conference 1993 Series (unpublished).
[14] D. Bahatt, O. Chesnovsky, and U. Even, Z. Phys. Chem. (in press).
[15] F. Merkt, S. R. Mackenzie, R. J. Rednall, and T. P. Softley, J. Chem. Phys. **99**, 8430 (1993).
[16] L. Ya Baranov, R. Kris, R. D. Levine, and U. Even, J. Chem. Phys. **100**, 186 (1994).
[17] W. G. Sherzer, H. L. Selzle, E. W. Schlag, and R. D. Levine, Phys. Rev. Lett. **72**, 1435 (1994).
[18] E. Rabani, L. Ya Baranov, R. D. Levine, and U. Even, Chem. Phys. Lett. (in press).
[19] D. Klar, K. Harth, J. Ganz, T. Kraft, M.-W. Ruf, H. Hotop, V. Tsemekhman, K. Tsemekhman, and M. Ya. Amusia, Z. Phys. D **23**, 101 (1992).
[20] R. G. Tonkyn, J. W. Winniczek, and M. G. White, Chem. Phys. Lett. **164**, 137 (1989).
[21] K. S. Haber, Y. Jiang, G. Bryant, E. R. Grant, and H. Lefebvre-Brion, Phys. Rev. A **44**, R5331 (1991).
[22] W. Kong, D. Rodgers, and J. W. Hepburn, J. Chem. Phys. **99**, 8571 (1993).
[23] H. A. Bethe and E. E. Salpeter, *Quantum Mechanics of One-and Two-Electrons Atoms* (Springer, Berlin 1957).
[24] M. L. Zimmerman, M. G. Littman, M. M. Kash, and D. Kleppner, Phys. Rev. A **20**, 2251 (1979)
[25] T. F. Gallagher, L. M. Humphrey, R. M. Hill, and S. M. Edelstein, Phys. Rev. Lett. **37**, 1465 (1976).
[26] W. E. Ernst, T. P. Softley, and R. N. Zare, Phys. Rev. A **37**, 4172 (1988).
[27] H. H. Fielding and T. P. Softley, Chem. Phys. Lett. **185**, 199 (1992).
[28] C. Bordas and H. Helm, Phys. Rev. A **47**, 1209 (1993).
[29] *Rydberg States of Atoms and Molecules*, edited by R. F. Stebbing and F. B. Dunning (Cambridge University, New York, 1983).
[30] R. N. Zare, *Angular Momentum. Understanding Spatial Aspects in Chemistry and Physics* (Wiley–Interscience, New York, 1988).
[31] G. I. Nemeth, H. L. Selzle, and E. W. Schlag, Chem. Phys. Lett. **215**, 151 (1993).
[32] E. de Beer, W. J. Buma, and C. A. de Lange, J. Chem. Phys. **99**, 3252 (1993).
[33] L. Zhu and P. Johnson, J. Chem. Phys. **94**, 5769 (1991).
[34] F. Merkt, S. R. Mackenzie, and T. P. Softley, J. Chem. Phys. **99**, 4213 (1993).